Far-infrared optical properties
of tetrathiofulvalene-tetracyanoquinodimethane (TTF-TCNQ)

H. Basista, D.A. Bonn, and T. Timusk

Department of Physics, McMaster University, Hamilton, Ontario, Canada L8S 4M1

Johannes Voit

Physikalisches Institut, Universität Bayreuth, D-8580 Bayreuth, Germany

D. Jérome

Laboratoire de Physique des Solides, Université Paris–Sud, 91405 Orsay, France

K. Bechgaard

H.C. Oersted Institute, Universitetsparken 5, DK 2100 Copenhagen, Denmark

Polarized far-infrared reflectance measurements of single-crystal mosaics of TTF-TCNQ have been made at several temperatures above and below the metal-insulator transition temperature range (54–38 K). The optical conductivity and dielectric function from 15 to 900 cm^{-1} show that the metallic regime above 60 K departs significantly from Drude free-electron behavior; the optical conductivity below 300 cm^{-1} is depressed before sharply increasing to a dc intercept value of 1700 $\Omega^{-1}\,cm^{-1}$. This strongly suggests the presence of a pseudogap. Strong one-dimensional Peierls fluctuations and electron-electron interactions are discussed as possible causes of the pseudogap and it is suggested that interaction effects are observed at high temperature. Optical evidence of the phase transition between 60 and 37 K to the insulating state is a dramatic drop in the absolute reflectance below 30 cm^{-1} as well as a broad absorption at 120 cm^{-1} which gives rise to a sharp edge in the optical conductivity below 300 cm^{-1}. A sharp conductivity peak between 30 and 100 cm^{-1} is interpreted as a collective antiphase oscillation of the electron charge-density wave on the TCNQ stack against the hole charge-density wave on the TTF stack. The pinned sliding mode is not observed directly.

I. INTRODUCTION

The discovery of large dc electrical conductivity in TTF-TCNQ by Coleman et al.[1] some 15 years ago and the subsequent discovery of superconductivity[2] in quasi-one-dimensional $TMTSF_2PF_6$ led to intense activity in hopes of engineering a superconductor with a high critical temperature as result of an electronic mechanism in place of the conventional BCS phonon coupling.[3]

The transport and optical properties of the organic superconductors are unusual. There is a power-law variation of the resistance with temperature extending well below the Debye temperature where the phonon conductivity has frozen out and no temperature dependence is expected. Another unusual feature is the non-Drude behavior of the normal-state optical absorption in the infrared which is dominated by a strong temperature-independent midinfrared band whose origin is obscure. It is worthwhile to reexamine the classic one-dimensional system TTF-TCNQ since questions still remain about the optical properties.[4-7]

In contrast to the high dc conductivity the far-infrared conductivity of TTF-TCNQ is anomalously low. Since the conductivity rises again in the midinfrared a gap appears between the microwave region and the 300 cm^{-1} frequency range. This non-Drude behavior suggests a novel mechanism of charge transport, a model of a dynamic charge-density wave in the presence of a "pseudogap." The high-temperature region above the three-dimensional phase transition is regarded as a one-dimensional precursor regime where the $2k_F$ phonon softening associated with a Peierls-type distortion becomes stronger with decreasing temperature and a weak pseudogap slowly develops at low frequencies. In this picture, a sliding charge-density wave with a long but finite relaxation time is responsible for a metalliclike high conductivity at dc and microwave frequencies.

Additional evidence of an exotic mechanism of charge transport in TTF-TCNQ is the appearance of a series of sharp absorption features below the metal-insulator transition temperature at frequencies corresponding to totally symmetric, not normally optically active, internal modes of vibration of the organic molecules making up the chains. Rice et al.[8,9] have studied the effects

of coupling between the conduction electrons along the chain axis and the internal molecular vibrations. The change from metal to insulator should be clearly marked optically by a reflectance which becomes rich in the internal A_{1g} modes of the organic molecules in the chain. For photon energies below the semiconducting gap, absorption maxima will appear at these phase phonon frequencies while above the gap, "antiresonance" peaks will be present due to the interference between discrete phase phonon modes with the continuum of conduction electron states.

Some of the optical properties of the quasi-one-dimensional organic conductor TTF-TCNQ have remained controversial because results from different experimental groups are in disagreement. Some of the previous theoretical and experimental work will be reviewed here with particular emphasis on the determination of the absolute value of the reflectance, always a difficult experimental problem in the infrared.

The earliest reflectance measurements are in the near infrared[10,11] and indicate the presence of a Drude-like plasma edge at 6000 cm^{-1} for temperatures both above and below the metal-insulator phase transition with broad, low peaks at higher frequencies due to interband transitions. The metal-insulator transition has no effect on the optical properties at these high frequencies—over the temperature range 70–4.2 K the fit parameters from Bright et al. do not change. In other words despite the large changes in the dc conductivity the midinfrared conductivity is essentially temperature independent. To understand this discrepancy it is necessary to turn to low-temperature far-infrared measurements; the most recent of these by Tanner et al.[12] and by Eldridge and Bates[13,14] have the greatest relevance to this study.

Tanner et al. found that the reflectance of a mosaic of single crystals at 300 cm^{-1} and above increased in absolute value from 0.75 at 300 K to almost 1.0 at 34 and 25 K. As a consequence of the high reflectance the conductivity peak at 290 cm^{-1} (interpreted as the edge of the Peierls energy gap) increases in height from 1000 Ω^{-1} cm^{-1} at 300 K to 15 000 Ω^{-1} cm^{-1} at 25 K. These near-unity reflectances at the higher frequencies are unusual and one strongly suspects that this is due to an instrumental artifact, perhaps a loss of signal in the metallized reference measurements.[15] The bending at low temperature as a result of different thermal contractions between the surface layer of evaporated gold and the sample underneath is one such effect. Also, we have found, that measurements on high-reflectance metals may be affected by high signal intensities that lead to an overload of the bolometer used as the detector.

Another interesting feature in the data of Tanner et al. is a sharp rise in the conductivity near dc at 60 K which develops into a broad peak between 50 and 100 cm^{-1} at 34 and 25 K. This is interpreted as the pinned charge-density wave that develops below the metal-insulator phase transition. Using the oscillator strength sum rule from dc up to 80 cm^{-1} the charge-density-wave effective

mass is estimated as $60m_e$. The dielectric function near dc for 60 K and higher temperatures is large and negative as expected for a metal and below 60 K it becomes positive as expected for an insulator. At 34 K ϵ_1 at dc is 6000, a factor of 2 higher than microwave measurements,[16] but at 25 K it is 3000 which is in good agreement.

A problem with the low-frequency extrapolation of reflectance at 25 and 34 K is the use of a negative slope to reach the 0.93 dc value predicted from microwave measurements causing unphysical negative values for the low-frequency conductivity from the Kramers-Kronig transformation. These discrepancies are indications that the measured low-frequency reflectance is too high. Finally, the deep minimum in the reflectance that develops at 120 cm^{-1} for 25 K is responsible for the abrupt overall drop in the low-frequency conductivity below 250 cm^{-1}. However, this feature in the reflectance as well as a developing phase phonon peak at 300 cm^{-1} are significantly different from the features in the 34-K reflectance curve. The last in the series of phase transitions for TTF-TCNQ is known to occur at 38 K, the temperature at which one expects any changing features to be nearly fully developed. It seems likely that the actual sample temperatures are higher than indicated—possibly as much as 10 K according to the results to be presented here.

Eldridge and Bates have used sensitive bolometric methods to measure the reflectance of TTF-TCNQ in the insulating phase at 12 K. In the early work, they find reflectances higher than 0.95 below 100 cm^{-1} with a steady drop to 0.82 at 800 cm^{-1}. This produces a broad peak of less than 3000 Ω^{-1} cm^{-1} in the optical conductivity between 100 and 250 cm^{-1}. The deep absorption at 120 cm^{-1} and the peak at 300 cm^{-1} are present in agreement with Tanner et al. but there is no near-unity reflectance at high frequency. In the more recent work, the reflectance above 100 cm^{-1} is lower than 0.90 with a flatter overall slope causing the broad peak in the conductivity to now be between 200 and 500 cm^{-1}.

Below 100 cm^{-1}, there are sharp narrow resonances in the low-frequency optical conductivity. However, a negative slope extrapolation to the dc reflectance of 0.93 again produces unphysical negative conductivities at low frequency. In the later work of Eldridge and Bates the measured structure at low frequencies is unchanged but the absolute reflectance has dropped by about 2% which causes a decrease in intensity of the narrow peak at 40 cm^{-1} in the conductivity by a factor of 3. This uncertainty of the reflectance level in the far infrared along with the necessity of an unphysical negative slope extrapolation is good reason to doubt the interpretation of this peak as evidence of a pinned charge-density wave.

Recent work of Gorshunov et al.[17] with a backward wave oscillator in the 8–30 cm^{-1} region strengthens the pseudogap picture of the transport at low frequency. At high temperature the 8-cm^{-1} conductivity is fairly close to the dc value but somewhat lower. As the temperature is lowered the millimeter wave conductivity drops while the dc conductivity is still rising. This is clear new

evidence of the narrowing of the collective mode responsible for charge transport at high temperature discussed by Tanner et al.[12] Below 38 K the 8-cm^{-1} conductivity remains constant and a strong, heavily damped mode develops at 40 cm^{-1}.

In summary, the reflectance in the far infrared of single crystals of TTF-TCNQ could provide direct evidence of a pseudogap due to a Peierls-type lattice distortion along with a collective mechanism of charge transport. Despite considerable experimental effort by several groups, a consensus on the applicability of these ideas is lacking and this is directly due to difficulties in the experimental techniques. An accurate determination of absolute reflectance is essential for a knowledge of both the location and magnitude in the optical conductivity of the semiconducting absorption edge in the low-temperature phase.

The intent of the present experimental study is to repeat the polarized reflectance measurements in the far infrared (15–900 cm^{-1}) over the temperature range 85–1.2 K. These results will be combined with reflectance measurements at higher frequencies published by other groups to produce composite reflectance curves needed to calculate the optical constants using the Kramers-Kronig transform.

The main controversial point which the present work has resolved is the height of the absorption edge located at 290 cm^{-1} in the optical conductivity for the low-temperature insulating phase. Eldridge and Bates[13,14] using a bolometric technique at 12 K, have measured this to be 2000 Ω^{-1} cm^{-1} while Tanner et al.[12] using single-crystal polarized reflectance from 25 to 160 K, found it to be 15 000 Ω^{-1} cm^{-1} for the low-temperature phase. The low-temperature results presented here are largely in agreement with those of Eldridge and Bates while the high-temperature results are an improvement over those of Tanner et al. However, an intense resonance in the conductivity near 40 cm^{-1} which both groups have attributed to oscillations of a pinned charge-density wave is instead an artifact of measured reflectances higher than 0.96 below 50 cm^{-1}, which has been more properly determined here to be less than 0.88. This resonance is still present in our data though with significantly less strength (maximum conductivity 1200 Ω^{-1} cm^{-1}) than in previous publications (5000–15 000 Ω^{-1} cm^{-1}).[12–14] In Sec. V, we will also give a new interpretation to this feature.

II. EXPERIMENTAL PROCEDURES

Polarized reflectance measurements were made on two different crystal mosaics of TTF-TCNQ. One mosaic was constructed with crystals obtained from D.B. Tanner, University of Florida, the other with crystals which were grown at Orsay and Copenhagen. The Florida crystals were 5 mm×1.1 mm×97 μm and had a layer of gold on the underside from previous use. The surface of these crystals bore evidence of cracking and flaking due in part to effects of age and thermal cycling. Sample quality of the Orsay-Copenhagen crystals was much better by comparison. These were 7.3 mm×0.67 mm×64 μm; there was no evidence of surface damage and they were not previously used.

The sample mount consisted of a 0.075-mm-thick brass sheet with a hole 3 mm×3 mm square cut through the center. With care being taken to minimize gaps between neighboring crystals the crystals were mounted across this hole and against the brass sheet to present a nearly uniform mosaic surface height to the beam. Glue was applied at one end only to avoid stresses. When handling single crystals, elaborate precautions are necessary to avoid shear forces or any mechanical shock that will crack or shatter the delicate crystals. The use of a vacuum tweezer is recommended. The estimated gap to crystal surface ratio for the successfully mounted mosaic made up of the Orsay-Copenhagen crystals is 3.5%.

The apparatus used for the polarized reflectance experiments has been described before.[18] The sample mount is attached to a brass light pipe probe held inside an evacuable space which is surrounded by a bath of liquid helium. The sample mosaic is mounted in a holder backed by a cavity lined with microwave absorbing foam. A polarizing grid is mounted on a 0.25-in. inner diameter tube which is capped by a square hole to minimize depolarization due to multiple reflections or focusing. Reflected intensity at 15° to the normal is measured by a composite germanium bolometer detector operating at 0.3 K. A bolometer bias voltage of 8 V was sufficient to prevent any problems with enhanced reflectance at high frequencies.

Significant improvements over the basic design of the probe have been made[19] by including an evaporator basket inside the anticryostat chamber. With this addition, it is possible to evaporate, in situ, at 85 K, a layer of metal with near 100% reflectance in the infrared (in this case lead) on the surface of the sample to provide an accurate absolute reflectance. The importance of the lead evaporation step is illustrated in Fig. 1. A kinematic sample mount has greatly improved the reproducibility of sample positioning.

Spectra in the far-infrared frequencies from 15 to 120 cm^{-1} were measured using a step and integrate Martin-Puplett polarizing interferometer while spectra in the range 120–900 cm^{-1} were measured using a continuous scanning Michelson interferometer with the output measured as an ac signal.

In any determination of optical constants of solids the accuracy of the absolute level of reflectance is a vital concern. To test the overall system several calibration tests were performed. We studied several well understood systems with optical conductivities whose magnitude approximated the TTF-TCNQ system. One of these was stainless steel which we assumed followed Drude theory. We measured the absolute reflectance of this material as a function of temperature and obtained agreement to 1% in the measured absolute reflectance and the calculated Drude value based on the measured dc conductivity as a function of temperature. Another system used for calibration was the heavy-fermion material UBe_{13} where we
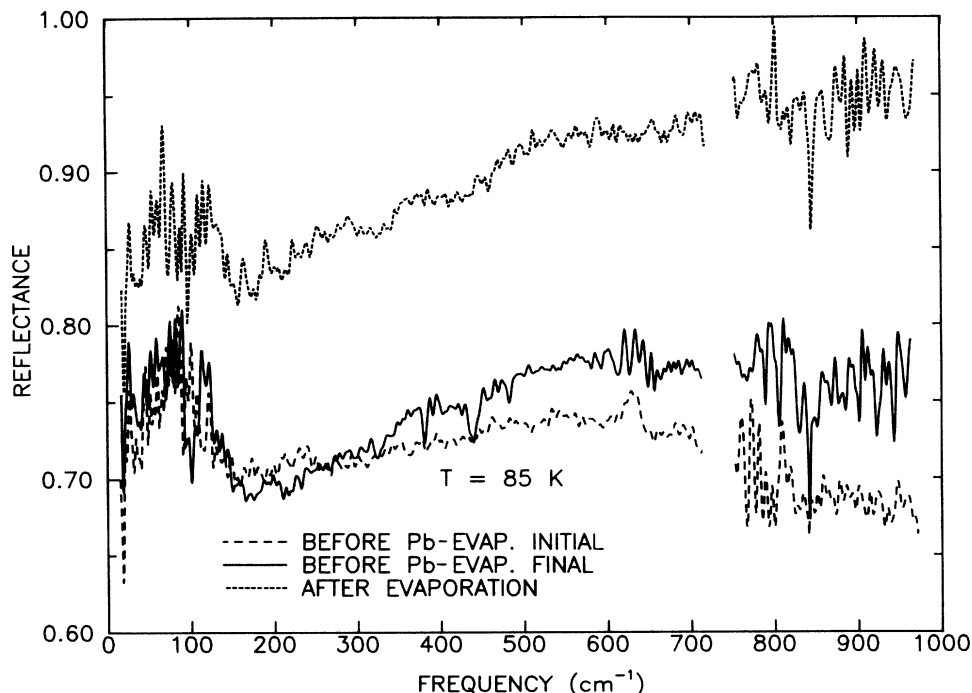
FIG. 1. Reflectance at 85 K of the TTF-TCNQ mosaic made from the newer crystals described in the text. The curve labeled "final" was measured after thermal cycling twice to room temperature after the "initial" measurement. The ratio of the curve before the evaporation to the curve after the evaporation represents the absolute reflectance of TTF-TCNQ.

again obtained, at high temperature where the anomalous optical effects are minimal, excellent agreement between the dc conductivity and the optical conductivity calculated from Drude theory.

III. RESULTS AND ANALYSIS

Reflectance curves are presented in Figs. 2–4 for 85, 60, 40, 37, and 1.2 K using the mosaic of newer Orsay-

Copenhagen crystals and for 85 K using the mosaic of older crystals from Tanner. After collecting a full temperature dependence of the reflectance, the lead evaporation was performed in the sample chamber at 85 K to establish an accurate absolute reflectance level. Ideally, thermal cycling should be limited to temperatures below 100 K but for the experiments on both sample mosaics, various problems required that the equipment be warmed up to room temperature for repairs. For the experiment
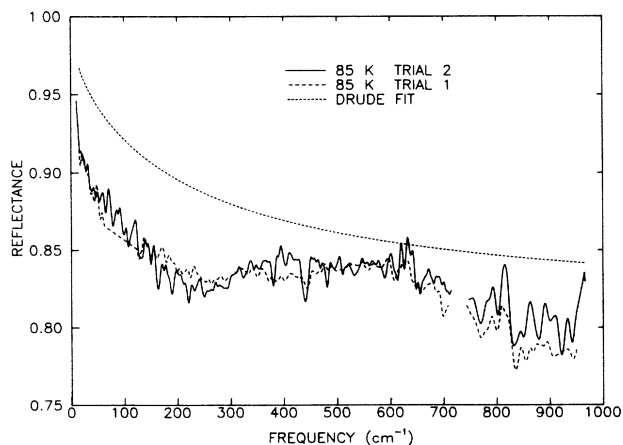

FIG. 2. Reflectance of TTF-TCNQ at 85 K compared to the Drude theory with the fitted parameters of Bright *et al.* (Ref. 18). The curve labeled "Trial 2" is the measurement on the mosaic of Orsay-Copenhagen crystals and the "Trial 1" curve is the measurement on the mosaic of crystals from Tanner.
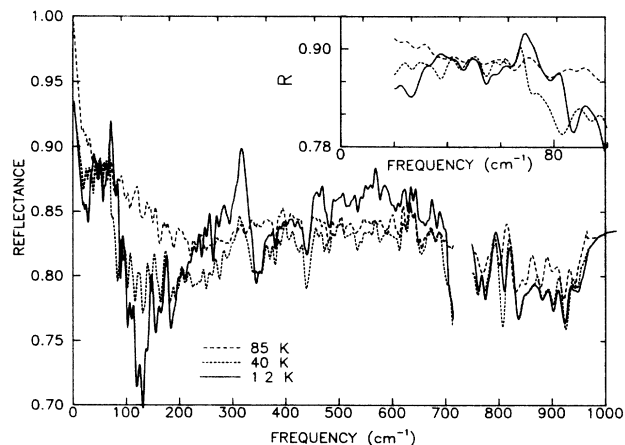

FIG. 3. Reflectance of TTF-TCNQ at 85, 40, and 1.2 K representing temperatures above and below the metal-insulator transition (38–54 K). The transition to the insulating state is marked by a drop in the reflectance below 30 cm^{-1}, a broad absorption at 120 cm^{-1}, and the appearance of activated phase phonon absorptions.
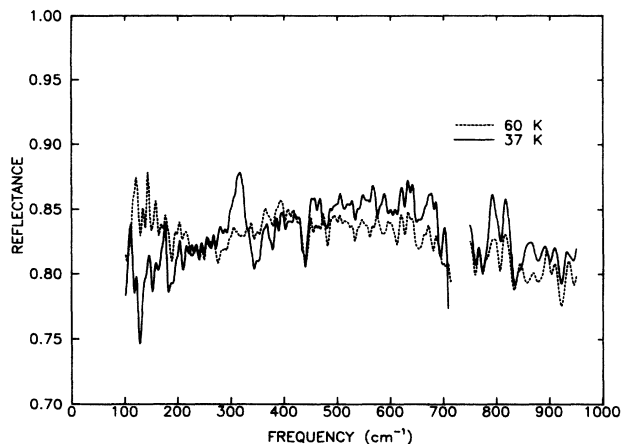
FIG. 4. Reflectance of TTF-TCNQ at 60 and 37 K show the features characteristic of the insulating state in intermediate stages of development.

with the mosaic of new crystals, this thermal cycling occurred twice. In both cases, the sample reflectance on the day of the evaporation increased (see Fig. 1) compared with measurements made before warming to room temperature. For the experiment with the mosaic of new crystals, a correction was possible by using the changes in reflectance with temperature, i.e., thermoreflectance, relative to the absolute reflectance at 85 K on the day of the lead evaporation to get absolute reflectances at all temperatures. However, this correction was not possible with the experiment on the mosaic of older crystals because the resolution was not chosen the same at all temperatures and only the 85 K reflectance is shown. This rise in reflectance after thermal cycling is not likely due to a change in the sample properties but rather to a change in the sample position. The crystals of the mosaic are fixed at one end only and a change in position of any of the crystals making up the mosaic will change the gap size and, consequently, the leakage through the mosaic.

The confidence limits of the absolute reflectance as estimated from reproducibility from scan to scan is better than 1% in the regions of maximum intensity of our spectrometer but is 3% above 750 cm^{-1} due to lower intensity in this frequency region.

The noise levels were highest in the overlap region for the two spectrometers from 80 to 120 cm^{-1} and the many divisions necessary to get absolute reflectance from thermoreflectance aggravated the problem further. A wide smoothing function was used in this region to reduce the noise to a level comparable with the surrounding regions. A gap in the data at 750 cm^{-1} in all the curves is due to a strong polyethylene absorption originating in the vacuum windows.

At 85 K, the deviation from Drude behavior (using the fitted parameters of Bright et al. shown in Fig. 2), is evident in the broad absorption below 300 cm^{-1} followed by a change in slope to meet the Drude curve at higher frequencies. Although TTF-TCNQ is metallic at this temperature (in fact, the dc conductivity is near maximum) this broad absorption indicates that some kind of gap in the low-frequency conductivity is present already.

Unlike the data of Tanner et al., the reflectance at this temperature does not reach near-unity values but is everywhere below the Drude reflectance. At 60 K, the absolute reflectance has not changed significantly but narrow absorption features are apparently beginning to develop at 275 and 350 cm^{-1}.

At 40 K, a dramatic 5% drop in reflectance from 120 to 250 cm^{-1} as well as a developing asymmetric peak at 317 cm^{-1} due to the TCNQ phase phonon indicates that a phase transition has occurred between 60 and 40 K. Also, the 3% drop in reflectance below 30 cm^{-1} is consistent with a metal to insulator transition. The high reflectance in the far infrared characteristic of metals reaches the value of unity at dc while, in the insulating state, the reflectance is extrapolated to the lower dc value of 0.93 using the microwave dielectric constant measured as 3200. At this temperature, it becomes possible to distinguish the changing line shapes near the predicted phase phonon frequencies.[20] Most noticeable are the peaks due to TTF located at 253 and 470 cm^{-1} and the peaks due to TCNQ located at 317 and 567 cm^{-1} with the phase phonons at 740 cm^{-1} due to TTF and at 726 cm^{-1} due to TCNQ missing in the gap caused by the polyethylene absorption.

Below 40 K, there is an abrupt rise in the height of the TCNQ phase phonon peak at 317 cm^{-1} accompanied by a 4% overall increase in the reflectance between 400 and 700 cm^{-1} above the 85 K level. The absorption edge below 250 cm^{-1} becomes more fully pronounced and, at 1.2 K, the absorption below 30 cm^{-1} reaches a full 6% below the 85 K level indicating that the transition to the insulating phase is complete.

The reflectance levels below 80 cm^{-1} in this work make it clear that extrapolations to the dc value of 0.93 in the insulating state do not need to have a negative slope as found by Eldridge and Bates and by Tanner et al. The development of the absorption edge below 200 cm^{-1} through the metal-insulator transition indicates the presence of a pseudogap in the low-frequency conductivity which is in agreement with both of these groups. The good agreement with Eldridge and Bates at low temperature is good reason to be confident of the higher-temperature results which are not in good agreement with the absolute reflectance of Tanner et al. Their near-unity reflectance at 700 cm^{-1} will cause a serious mismatch with the measurements by Tanner[21] which have a 0.87 reflectance at 800 cm^{-1} and are dropping at lower frequencies. The mismatch is only 4% above the level measured here. Also, changes in the reflectance curve occur at temperatures consistent with the expected critical temperatures determined by other techniques. In particular, notice that the reflectance curve labeled 34 K in the work of Tanner et al. is similar to the curve labeled 40 K in this work.

IV. THE OPTICAL CONDUCTIVITY AND DIELECTRIC FUNCTION OF TTF-TCNQ

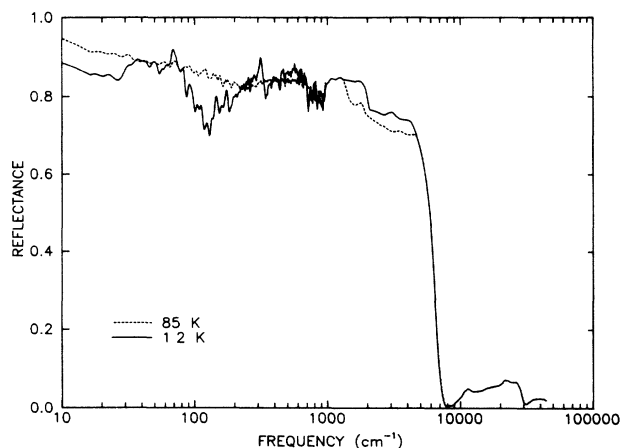The far-infrared measurements of this study cover the frequency range 15 to 800 cm^{-1}. To perform Kramers-

FIG. 5. The full composite reflectance of TTF-TCNQ (note the logarithmic scale in frequency) used in the Kramers-Kronig transform at 85 and 1.2 K.

Kronig analysis it is necessary to extend the measurements to low and high frequencies. Below 15 cm^{-1}, the reflectance is linearly extrapolated to unity for temperatures above the metal-insulator transition, i.e., at 60 and 85 K, while, in the insulating phase, the dc reflectance is estimated as 0.93 from the microwave measurement of the dielectric constant[16] ($\epsilon_1 = 3200$, $\epsilon_2 \simeq 0$ at 10 GHz). The reflectances of the 60- and 37-K data below 100 cm^{-1} were estimated using the 85- and 40-K data, respectively. Above 800 cm^{-1}, Tanner's measurements[21] for 60 and 25 K are used to 4000 cm^{-1} although these were multiplied by a factor of 0.93 to match the upper limit of uncertainty of the 800-cm^{-1} reflectance of this study. In the region of the plasma absorption the reflectance is calculated from the Drude fit of Bright et al.[11] and the reflectance in the interband region up to the visible is taken from Grant et al.[10] Above this range, the reflectance is estimated using the equation $R(\omega) = c\omega^{-4}$ and its contribution to the phase can be calculated analytically. Figure 5 illustrates the resulting reflectance at two temperatures.

The real part of the optical conductivity, determined by Kramers-Kronig transformations at all measured temperatures is presented in Figs. 6–9. At 85 K, the shape and magnitude is in good agreement with the Drude conductivity above 300 cm^{-1} (Fig. 6), but below this frequency is a region of depressed conductivity which is suggestive of the Lee, Rice, and Anderson[22] picture of a developing pseudogap. The shape of the conductivity below 15 cm^{-1} is sensitive to the choice of extrapolation to dc in the reflectance. The reflectance of metals in the far infrared can often be approximated by the Hagen-Rubens formula, $R(\omega) = 1 - \sqrt{2\omega/\pi\sigma_{dc}}$, but, in this case, an artificially high σ_{dc} must be used to force a match at 15 cm^{-1} and the resulting conductivity below 15 cm^{-1} is a constant 290 Ω^{-1} cm^{-1}. On the other hand, a linear extrapolation to unity causes a steep upturn to a high dc conductivity intercept and, although somewhat arbitrarily, this is taken as the better choice. These choices
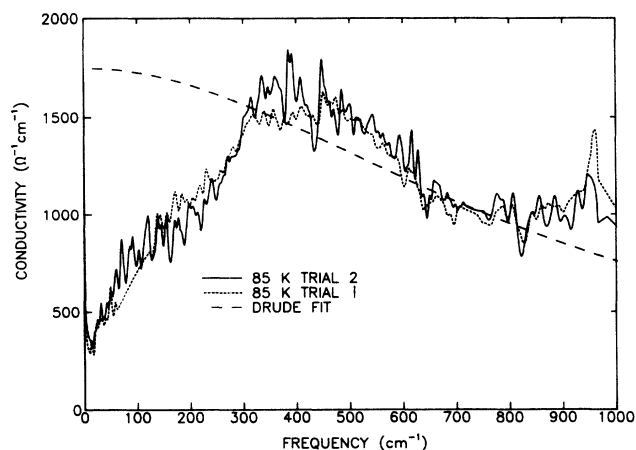

FIG. 6. Real part of the optical conductivity of TTF-TCNQ at 85 K along with the Drude curve using the fitted parameters of Bright et al. (Ref. 18). Again, the "Trial 2" curve represents the measurements on the mosaic using the crystals from Paris while the "Trial 1" curve is the measurement on the crystals from Tanner.
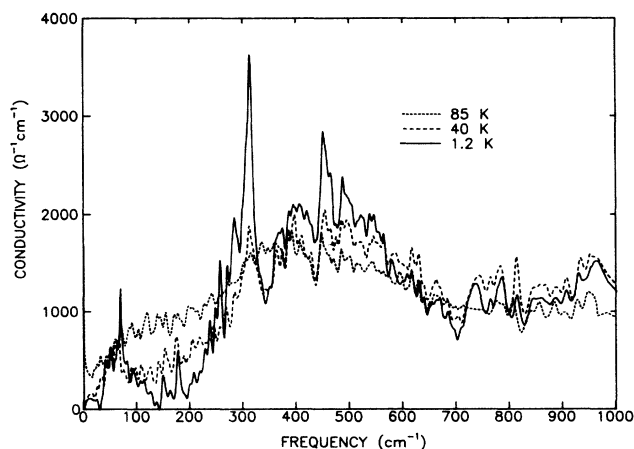

FIG. 7. Real part of the optical conductivity of TTF-TCNQ at 85, 40, and 1.2 K representing temperatures above and below the metal-insulator transition. Note that the dominant features are the developing absorption edge near 300 cm^{-1} and the TCNQ phase phonon indentation at 317 cm^{-1}.
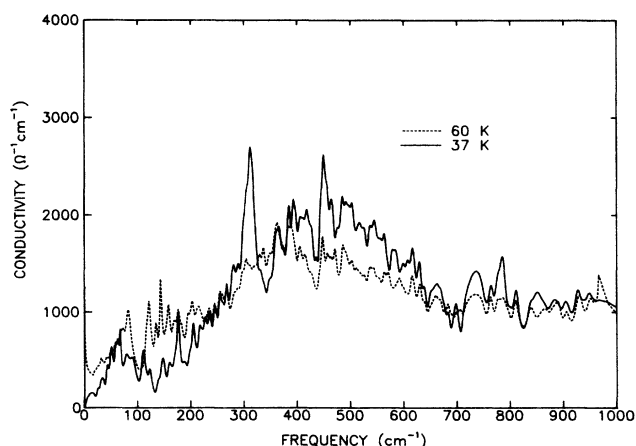

FIG. 8. Real part of the optical conductivity of TTF-TCNQ at the intermediate temperatures 60 and 37 K.
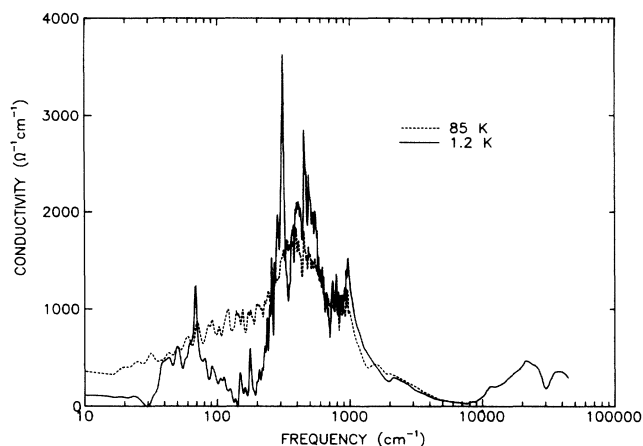
FIG. 9. Real part of the optical conductivity of TTF-TCNQ at 85 and 1.2 K over the full frequency scale used in the Kramers-Kronig transform (note the logarithmic scale in frequency).

do not noticeably affect the conductivity above 15 cm^{-1} and the zero frequency peak caused by the linear extrapolation should not be regarded as evidence of a collective mode. It is interesting to note, however, that the dc conductivity intercept of the newer crystals is 1700 Ω^{-1} cm^{-1} while that of the older crystals is only 1100 Ω^{-1} cm^{-1}.

As the temperature is lowered below the metal-insulator transition, the conductivity below 300 cm^{-1} rapidly drops below the level of the metallic regime as the pseudogap develops into a true gap. Accompanying this is the development of a large phase phonon "antiresonance" indentation in the conductivity at 350 cm^{-1} as well as the activated absorption peaks at 160 cm^{-1} and 180 cm^{-1}.

The low-temperature optical conductivity above 300 cm^{-1} is in good agreement with the work of Eldridge
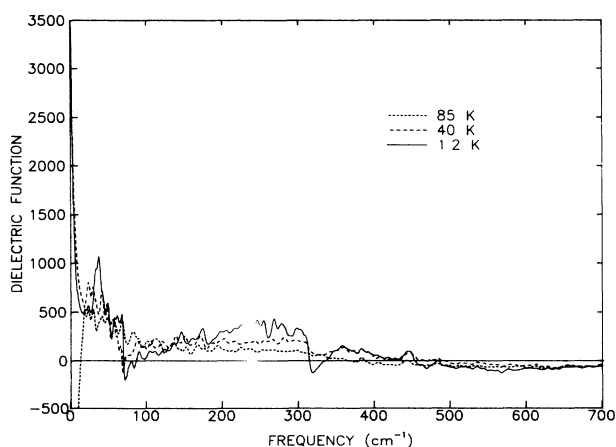

FIG. 10. Real part of the dielectric function of TTF-TCNQ above and below the metal-insulator transition. Note that the dc intercept changes from large negative values in the metallic regime to positive values that are in good agreement with microwave measurements (Ref. 21).
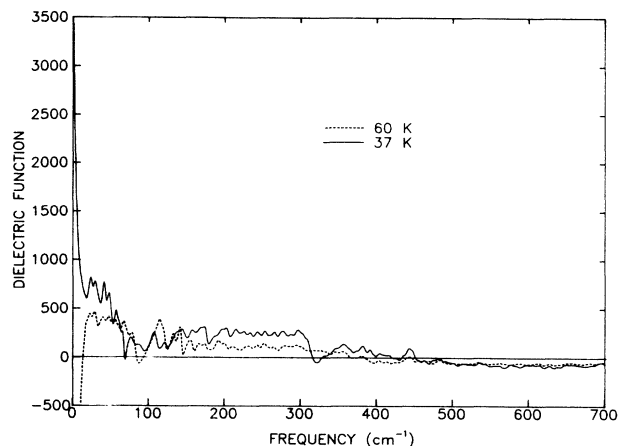

FIG. 11. Real part of the dielectric function of TTF-TCNQ at the intermediate temperatures 60 and 37 K.

and Bates although the higher resolution above 120 cm^{-1} in their study has resulted in a sharper, better resolved peak at the absorption edge. This represents an important consensus among two groups in the determination of this peak height and strongly suggests that the 15 000 Ω^{-1} cm^{-1} resonance in the work of Tanner et al. is due to an instrumental artifact.

At frequencies below 110 cm^{-1}, there is an enhanced region of conductivity which does not reach peak values of 5000 Ω^{-1} cm^{-1} as indicated by Eldridge and Bates and by Tanner et al. as due to a pinned charge-density wave sliding mode. These high peak values are an artifact of reflectances below 50 cm^{-1} that reach above 0.96 and, instead of a high peak, the same feature here has caused a minimum in the conductivity at 35 cm^{-1}. The lower reflectance value here also means there is no nonphysical negative conductivities at low frequencies due to a negative slope low-frequency extrapolations in the reflectance.

The optical conductivity at 85 and 1.2 K in the full frequency range of interest, shown in Fig. 9, illustrates the high-frequency metallic behavior of this material both above and below the metal-insulator transition.

The dielectric function at the lowest frequencies changes from a large and negative value in the metallic regime to a smaller positive value in the insulating phase (see Figs. 10 and 11). At 40 K, the dc dielectric constant is 3400 while at 1.2 K it is 3200 which is in good agreement with microwave measurements. Below 300 cm^{-1}, there is an anomalously high dielectric constant both above and below the metal-insulator transition while, above 600 cm^{-1}, the dielectric constant is small and negative, which is characteristic of metals.

V. DISCUSSION

In this section, we will discuss the main issues raised by the experiments: (i) the origin of the depressed conductivity below 300 cm^{-1}, (ii) the nature of the peak be-

tween 30 and 110 cm^{-1}, and (iii) the absence of a sharp gap structure even at the lowest temperatures.

In the frequency range $\omega \ll \tau^{-1}$ with τ the scattering time of the Drude model, the optical conductivity directly probes the density of states around the Fermi level; our measurements thus suggest a strongly depressed density of states at low frequency already at the highest temperature experimentally accessible (85 K) *despite* a high dc conductivity.

Lee, Rice and Anderson[22] (LRA) first suggested the possibility of a "pseudogap" in the density of states due to strong one-dimensional (1D) fluctuations. They considered a 1D electron-phonon system without electron-electron interactions. Fluctuations prevent the system from ordering at the mean-field temperature T_{MF}. Rather, T_{MF} sets the temperature scale below which effects of the Peierls ordering appears through a depressed density of states at the Fermi level. In a strictly 1D system, this pseudogap deepens with decreasing temperature until it develops into a full gap at $T = 0$ while in the presence of transverse coupling, a full gap develops already at a finite temperature $T_c < T_{MF}$. From 85 to 40 K, our data are only in rough agreement with this picture.[23]

An alternate view would be to describe the optical conductivity of TTF-TCNQ and other organic conductors by a low background conductivity with a significant enhancement taking place in the region above ~ 300 cm^{-1}; Holstein phonon emission[24] was proposed as a possible mechanism responsible for this enhancement.[11,25] Also charge transfer or excitonic bands are compatible with an absorption in this frequency range. Specifically, the latter two mechanisms have been discussed in the context of a midinfrared absorption of very similar shape and temperature (in-)dependence occurring in the high-T_c copper oxides. Another possibility is an interband absorption in the vicinity of a point Fermi surface generated by strong electron-electron interactions; such a mechanism has been discussed recently for the high-T_c materials[26] and can be extended to more anisotropic systems such as TTF-TCNQ.[27]

The discussion of the optical conductivity of TTF-TCNQ is significantly complicated by the two chains available for conduction which order at different temperatures. It is then important to have independent information the order of magnitude of fundamental interaction parameters (electron-electron and electron-phonon) which determine the physical behavior of the system, at least in the framework of simple models. We therefore briefly review further experimental information allowing such estimates. An analysis of the temperature dependence of the phason activated totally symmetric intramolecular vibrations[28] indicates that the 54-K transition only affects the TCNQ stack. TTF begins to order below 49 K; the fact that thermodynamic and transport measurements are most seriously affected only below 38 K suggests that the gap on the TTF stack exceeds $k_B T$ only for $T < 38$ K. $2k_F$ precursor effects are observed up

to 150 K; in addition, $4k_F$ charge-density-wave (CDW) correlations have been observed even at room temperature, becoming sharp below 150 K.[29] Theoretical attempts to explain this anomaly all invoke strongly repulsive interactions between electrons.[30] From temperature-dependent interferences between $2k_F$ and $4k_F$ modulations, the $4k_F$ CDW can be assigned to the TTF stack.[31] Further evidence for strong Coulomb interactions comes from independent experiments, such as the room-temperature value of the Pauli susceptibility or the Korringa enhancement of the NMR relaxation rate.[32] Generally, it is agreed upon that the ratio $U/4t$ of a Hubbard on-site repulsion and the intrachain bandwidth is of the order of unity with bandwidths of the order 0.75 eV. There is also a consensus that $U/4t$ should be larger on the TTF stack than on the TCNQ stack, while the relative magnitude of the bandwidths is subject to discussion.

Contrary to the situation encountered in three-dimensional metals, where the density of states at the Fermi level $N(\omega)$ is largely independent of the interactions between electrons, in 1D systems it depends sensitively on electron-electron and electron-phonon coupling. In an interacting 1D electron gas, $N(\omega)$ at low ω is strongly depressed with respect to a noninteracting system. Again, this is a pseudogap; however, its shape is quite different from the one proposed by Lee, Rice, and Anderson.

More precisely, in the weak-coupling theories of the 1D electron gas where the Coulomb interactions are parametrized by coupling constants g_i,[33] the density of states close to the Fermi level at zero temperature is given by[34]

$$N(\omega) \sim \omega^{(C_\rho + C_\sigma)/4} , \quad g_1 \geq 0 , \tag{1}$$

$$N(\omega) \sim | \omega - \Delta_\sigma |^{C_\rho/4 - 1/2} , \quad g_1 < 0 . \tag{2}$$

In these expressions,

$$C_\nu = 2[\cosh(2\xi_\nu) - 1] , \tag{3}$$

$$\exp(4\xi_\nu) = \frac{\pi v_F - g_{2,\nu} + g_{1,\parallel}/2}{\pi v_F + g_{2,\nu} - g_{1,\parallel}/2} \quad (\nu = \rho, \sigma). \tag{4}$$

v_F denotes the Fermi velocity, $g_{2,\nu}$ the forward scattering (momentum transfer $q \approx 0$) coupling constant for the charge ($\nu = \rho$) and spin ($\nu = \sigma$) density degrees of freedom, and $g_{1,\parallel}$ is the backward scattering (momentum transfer $q \approx 2k_F$) constant for parallel spin scattering. We have only exhibited the expressions applying to incommensurate systems such as TTF-TCNQ. The density of states $N(\omega)$ expected from Eqs. (1) and (2) is displayed in Fig. 12. The full line applies to vanishing backward scattering; this case is relevant for repulsive interactions which, for spin-isotropic interactions, renormalize towards $g_{1,\parallel}^* = g_{1,\perp}^* = 0$. Charge and spin fluctuations are gapless then. If the backward scattering
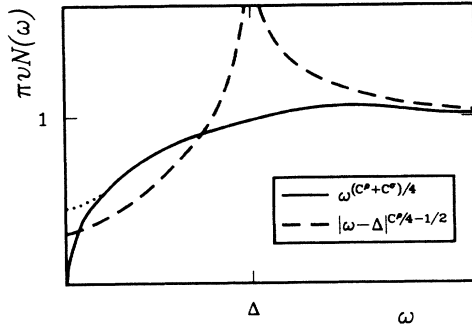
FIG. 12.   Pseudogap in the density of states $N(\omega)$ of a 1D electron gas with repulsive (solid line) and attractive (dashed line) interactions, after Ref. 39.

is attractive, the charge-density fluctuations will remain gapless, while a gap (Δ_σ) opens in the spin-density excitations and we must use Eq. (2). Equations (1) and (2) were derived for zero temperature; the essential effect of finite temperature is to fill up the extreme low-frequency part of (1) for $g_1 \geq 0$;[34] this is indicated by the dotted line in Fig. 12. For $g_1 < 0$, finite T presumably smears the divergence at $\omega \sim \Delta$. Note that expression (4) is model dependent and universal only to lowest order in the coupling constants; hence reliable estimates can only be obtained for weak coupling.

It is important to note that only at very high temperatures (of the order of the Fermi energy), can bare coupling constants g_i be used in Eq. (4); at lower temperatures, renormalized effective interaction constants enter our Eqs. (1)–(4). There are several sources for such renormalizations. An important one is the (attractive) electron-phonon interaction. In particular, it has been demonstrated[35] that electron-phonon interaction may cause a crossover from a regime where the system is dominated by repulsive interactions to one where the interactions behave effectively attractive as the energy scale (e.g., temperature) is lowered. Then, a Peierls instability may occur. In such a case, (2) applies and it is interesting to note that this density of states bears some resemblance to the one derived by LRA.[22]

The depressed low-frequency conductivity in the spectrum taken at 85 K is extremely reminiscent of the pseudogaps discussed above. Apart from the bump in the 300–600 cm^{-1} region, we have a flat background which appears to drop as a power law at low frequencies. The behavior at frequencies below 15 cm^{-1} depends on the low-frequency extrapolation procedure chosen, as previously discussed. However, from the work of Gorshunov et al.,[17] which in nearly all aspects is consistent with the present work, we expect a further decrease of the conductivity below 15 cm^{-1}: indeed, from their Fig. 1, one would obtain $\sigma(10$ cm$^{-1}) \sim 100$ Ω^{-1} cm^{-1} at 85 K, a conductivity significantly lower than the conductivity minimum of 300 Ω^{-1} cm^{-1} at 15 cm^{-1} in our data. The observed behavior is compatible with Eq. (1) and the importance of repulsive interactions. Moreover, since the temperature T_x where 3D correlations become important

is estimated as $T_x \sim 60$ K,[36] the application of Eqs. (1) and (2) is justified. The observed form of the frequency dependence is compatible with $g_i/\pi v_F \sim 1$, i.e., relatively strong repulsive interactions ($U \sim 4t$ in the language of the Hubbard model), consistent with the independent information on TTF-TCNQ previously reviewed.

One might attempt a fit of the low-frequency spectrum to Eq. (1). Aside from the noise in $\sigma(\omega)$, leading only to a limited accuracy, there is a more fundamental problem with such a program: TTF-TCNQ is a two-chain conductor, and the conductivity is the sum of the conductivities of the individual chains. A decomposition into the TTF and TCNQ stack and an estimate of the renormalized interaction parameters from the exponents C_ρ and C_σ, which are certainly different on both stacks, are far from obvious. The presence of two chains also prevents a straightforward interpretation of the conductivity bump around 450 cm^{-1}. It may either be a contribution of a different conduction mechanism (such as Holstein phonon emission, cf. the following) or indicate a different functional form of the densities of states $N(\omega)$ on the two chains.

In this case, the low-frequency part ($\omega < 200$ cm^{-1}) would then be mainly due to one chain which is dominated by repulsive interactions and described by Eq. (1); most probably, this is the TTF stack on account of the $4k_F$ correlations observed. The enhanced conductivity in the intermediate-frequency range ($300 < \omega < 600$ cm^{-1}) would come from the second (TCNQ) chain; here, the density of states would be of the form of Eq. (2), hence the electrons would interact through an effectively attractive interaction. Since the TCNQ chain exhibits sizable $2k_F$ correlations at 85 K, the effective interaction between electrons has been renormalized (e.g., by phonons) to overall attractive behavior on TCNQ at 85 K. Indeed, in an incommensurate 1D system, an effectively attractive backscattering component ($g_1 < 0$) is necessary to favor charge- over spin-density-wave fluctuations. Δ_σ in Eq. (2) is then estimated of the order of 300 cm^{-1}. According to this picture, the pseudogap observed at 85 K would *mainly reflect the effective electronic interactions on both stacks.*

As the temperature is lowered, it is expected that the pseudogap on the TCNQ stack will develop into a real gap at 54 K. Precursor effects due to strong critical fluctuations as discussed by LRA should be visible up to the 3D coherence temperature $T_x \sim 60$ K,[36] at least. The TTF stack is expected to show a crossover from a pseudogap (1) to one of the LRA type at latest at 49 K and a full gap at 38 K (cf. the following). Our spectra qualitatively agree with this picture.

The main features of the optical spectrum of TTF-TCNQ at *any fixed temperature* are also compatible with the results of a recent theory of Holstein conduction in a 1D system in the presence of (repulsive) electron-electron interactions.[37] There, it was found that (i) only the electron-phonon backscattering processes ("g_1" in the preceding language) modify the optical conductivity,

and (ii) in the "metallic" state $\sigma(\omega) \propto \Theta(\omega - \omega_{2k_F})(\omega - \omega_{2k_F})^{1-\alpha}$ close to the phonon frequency ω_{2k_F}. The exponent α characterizes the decay of CDW correlations, and $\alpha > 0$ for repulsive interactions. The conductivity in the frequency region above 300 cm^{-1} can be described by these expressions assuming a phonon frequency of this order of magnitude. However, the variation of the spectrum as the temperature is lowered from 85 to 1.2 K suggests that the Holstein process is unlikely to be an important contribution. Specifically, the onset of Holstein conductivity should shift by 2Δ upon going from the metallic state into the semiconducting one, where 2Δ is the CDW gap. Both from the preceding discussion and from dc measurements, a gap of order 300 cm^{-1} was estimated. A corresponding shift is not observed in our experiment. On the other hand, one could argue (based on our previous discussion) that the system is far from ideally metallic at 85 K and already exhibits strong CDW fluctuations on both chains. Describing them by some local order parameter and thus gap, the system might "see" an effective gap Δ_{eff} already at 85 K. Still, Δ_{eff} should vary with T as it develops into a real gap at T_{cQ} or T_{cF}. It is then surprising that the quantity $2\Delta_{\text{eff}} + \omega_{2k_F}$, determining the onset of Holstein conductivity, would be independent of temperature between 85 and 1.2 K. This clearly points to the importance of performing optical measurements over a wide range of temperatures where significant changes in the electronic and crystallographic structure of a system might occur.

There is an interesting peak in the spectra at 60 K and below, between 30 and 110 cm^{-1}. Its amplitude is significantly smaller than in previous studies (cf. the preceding) where it has been attributed to the pinned sliding mode of the CDW.[12-14] In view of relations between pinning frequency ω_{pin} and threshold field E_T in simple models of CDW conduction[38] this assignment is implausible, however, (i) due to the small temperature dependence of this peak while E_T varies strongly below 60 K,[39] and (ii) due to the order of magnitude difference with estimates based on experimental threshold fields.[39]

The TTF chain containing holes and the TCNQ chain containing electrons undergo CDW transitions at 38 and 54 K, respectively. The electron and hole CDW's have opposite charges and therefore tend to move in opposite sense under the influence of an electric field. A Ginzburg-Landau functional for the free energy has been proposed to describe the response of the two-chain system, at least in the temperature range around the phase transitions, to an electric field E:[39,40]

$$f = f_0 + \lambda\rho_Q\rho_F \cos 2\phi_-$$
$$+(eE/\pi)[(\rho_{cQ} - \rho_{cF})\phi_+ + (\rho_{cQ} + \rho_{cF})\phi_-] \,. \quad (5)$$

Here, $\rho_F(\rho_Q)$ is the CDW amplitude on the TTF (TCNQ) chain, $\phi_\pm = (\phi_Q \pm \phi_F)/2$ with $\phi_F(\phi_Q)$ the CDW phases, and ρ_{cF} and ρ_{cQ} the fraction of the condensed carriers in the CDW. λ is the interaction between the CDW's, and f_0 describes the individual chains.

Note that there are *two collective modes* $\phi_\pm$ since the carriers condensed in the CDW's on the TTF and TCNQ stacks have different sign. The situation is sketched in Figure 13. ϕ_+ is the sliding CDW mode where both CDW's move in the same direction in an external field. This mode was believed to be observed in earlier experiments.[12-14] Although fluctuations of this mode are observed to contribute to the dc conductivity above the phase transition temperature, impurities should pin it at a finite frequency $\omega_{\text{pin},+}$. The impurity pinning, in principle, occurs separately on both chains and should be included in the f_0 term in Eq. (5), e.g., through a Hamiltonian as given by Fukuyama and Lee.[41] It has been demonstrated[39] that this mode can be depinned by a moderate electric field in the temperature range where only one CDW is fully ordered ($T > 34$ K). From the observed threshold fields[39] one can estimate a pinning frequency $\omega_{\text{pin},+} \sim 0.1$–1 cm^{-1}, orders of magnitude below our far-infrared feature. This mode should be present not only at 85 and 60 K, but also at 40 and 37 K though with less strength: from Eq. (5) one sees that it couples to the electric field only as long as $\rho_{cQ} - \rho_{cF} > 0$. When the temperature decreases below 38 K, the difference between the fractions of condensed carriers rapidly approaches zero; then ϕ_+ is no longer coupled to the electric field. Depending on the pinning frequency and the width of the ϕ_+ mode, it is conceivable that the conductivity at the pinning frequency is considerably higher than the observed dc conductivity.

ϕ_- is an "antiphase" mode where the two CDW's move in opposite direction under an applied electric field. This mode may be described as "self-pinned" by the Coulomb interaction between the electron and the hole CDW's on the two stacks. It carries an oscillating dipole moment and therefore is optically active. ϕ_- is the mode we believe to observe in our experiment in the 30–100 cm^{-1} range. From Eq. (5), we see that it couples to the electric field better, the more carriers are condensed into both CDW's, i.e., the lower the temperature. It may
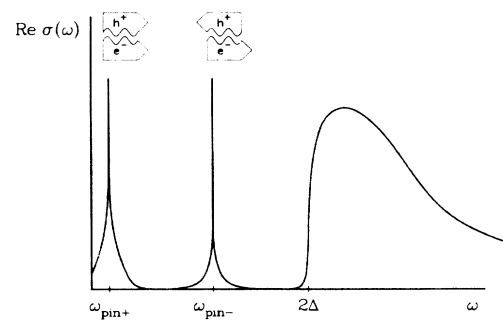

FIG. 13. Sketch of the optical conductivity of a CDW system involving electron and hole CDW's. The sliding mode ϕ_+ where both CDW's move in the same direction is pinned at $\omega_{\text{pin},+}$. The antiphase mode ϕ_- is pinned at $\omega_{\text{pin},-}$; both CDW's move in opposite directions. The features are not drawn to scale.

be present already above 54 K due to CDW fluctuations on both chains. The intensity of this mode should increase on lowering the temperature; this is observed in our experiment. The antiphase mode pinning frequency varies as $\omega_{\mathrm{pin},-} \propto \rho_{cQ}\rho_{cF}/(\rho_{cQ}+\rho_{cF})$. In a mean-field theory, $\rho_{cQ,F}$ are zero for $T > T_{cQ,F}$, respectively, and therefore $\omega_{\mathrm{pin},-} = 0$ for $T > T_{cF} = \min(T_{cQ}, T_{cF})$. In a theory including fluctuation effects, the temperature variation of $\omega_{\mathrm{pin},-}$ is much slower: $\omega_{\mathrm{pin},-}$ is expected to remain finite as long as there are $2k_F$ correlations on each chain, i.e., up to temperatures much higher than 54 K. It should increase slightly with decreasing temperature and saturate at low T. In the temperature range where this mode is observed clearly ($T \leq 40$ K) we do not expect a strong temperature dependence. Moreover, ϕ_- should be much less sensitive to weak impurities than ϕ_+. In Ref. 39 an order of magnitude for the antiphase mode pinning frequency $\omega_{\mathrm{pin},-}$ is obtained which is consistent with the present observation. Also Gorshunov et al.[17] found signatures of a peak with $\omega_{\mathrm{pin},-} \sim 40$ cm^{-1} in their submillimeter spectra and attributed it to antiphase oscillations.

While there is no direct signature of the sliding (ϕ_+) mode in the present experiments, the picture previously put forward might prove helpful in settling a puzzle arising from the comparison of different experiments. The extrapolation of the measured reflectivities (above 40 K) to zero frequency used in the present work would imply negative dielectric constants in the microwave region. The very same implication follows from the work of Gorshunov et al.[17] Direct measurements in the microwave region[42] however yielded extremely high positive values of order 2500 at room temperature and still higher values at helium temperature. Assuming a monotonous behavior below about 10 cm^{-1}, both Gorshunov's and our data are incompatible with the microwave dielectric constants above 40 K. On the other hand, if the microwave data are reliable, compatibility with the present work could only be restored by assuming an oscillator at extremely low but finite frequency not seen until now in the far-infrared and submillimeter work. The pinned ϕ_+ mode is such a possibility, in particular since the above estimates point to an $\omega_{\mathrm{pin},+}$ in the microwave range.

Surprisingly, we do not observe a sharp structure associated with the Peierls gap around 300–400 cm^{-1} even at 1.2 K. In an incommensurate single-chain CDW system, due to the sliding collective mode, the usual reciprocal square-root singularity in the density of states at 2Δ typical of "ordinary" 1D semiconductors is changed into a square-root edge singularity in the incommensurate CDW system with an additional δ function peak of relative strength m_e/m^* at the origin.[22] Here, m_e is the electron band mass and m^* the CDW mass. In TTF-TCNQ, based on a single-chain picture, Tanner et al.[12] estimated m_e/m^* of order $\frac{1}{60}$. Using the LRA results, one can estimate that in such a case, the edge singularity should be extremely sharp and extend up to a peak conductivity of about 2×10^5 Ω^{-1} cm^{-1} just above the electronic gap. This is not seen in the experiment. There are at least two factors contributing to a reduction of the height of the conductivity peak at 2Δ. (i) Tanner's estimate of the oscillator strength in the collective mode only accounts for that in the ϕ_- mode observed in the infrared. How much oscillator strength resides in the ϕ_+ mode at much lower frequencies is unknown. (ii) Also the phason activated intramolecular vibrations below or close to the edge of the gap with their rather broad wings (especially the TCNQ vibration at 317 cm^{-1}) will transfer conductivity from above to below the gap edge and thereby effectively smear the gap structure. A similar absence of a sharp gaplike structure is observed in the optical conductivity of 1:2 TCNQ salts[43] which are successfully described by Rice's theory.[9] Note however, that in these salts, the maximum conductivities measured above the gap are typically a factor 5 lower than in TTF-TCNQ while the gap is a factor 5 larger. It would be very interesting to have an extension and a combination of the theories of Rice and Lee, Rice, and Anderson for incommensurate two-chain CDW systems in order to attempt a detailed fit to the low-temperature conductivity of TTF-TCNQ.

VI. CONCLUSIONS

The far-infrared optical conductivity of TTF-TCNQ in the high-temperature metallic regime reveals the presence of a pseudogap below 300 cm^{-1}. Using a value of 290 cm^{-1} for the energy gap, mean-field theory yields the value $T_c = 120$ K which is a factor of 2 higher than the observed metal-insulator transition temperature. It is interesting to note, however, that structural studies[44] reveal the $2k_F$ lattice distortion beginning to develop noticeably at 150 K. These high temperatures are out of range of the apparatus used here in its present form.

There is no clear evidence of a zero frequency mode above 15 cm^{-1}; the behavior below 15 cm^{-1} depends on the choice of low-frequency extrapolation. The rapid drop in conductivity inside the developing Peierls semiconducting gap at 40 K and below is accompanied by the development of activated phase phonon absorptions, which further supports the widely held claim that TTF-TCNQ is in a static charge-density-wave state below 40 K. The prominence of the TCNQ phase phonons over those of TTF suggests that the conductivity is primarily along the TCNQ chains. The insulating phase of TTF-TCNQ shows interesting similarities with a related TCNQ linear chain organic, TEA(TCNQ)$_2$,[45,46] which is already semiconducting at room temperature. This material exhibits a semiconducting gap at 1000 cm^{-1} and also shows activated absorptions inside the gap with phase phonon indentations in the conductivity above the gap.

The results of this study have clarified some of the experimental problems with recent reflectance measurements on TTF-TCNQ. The low-temperature conductivity results of Tanner et al., which indicate the devel-

opment of a peak absorption edge of $15\,000$ $\Omega^{-1}\,cm^{-1}$, is an artifact of near-unity reflectance above 500 cm^{-1}. The lower peak conductivity value of 2000 $\Omega^{-1}\,cm^{-1}$ determined by Eldridge and Bates is in good agreement with the results of this study. However, the strong peak resonance of 5000 $\Omega^{-1}\,cm^{-1}$ at 35 cm^{-1} which both of these groups claim is due to oscillations of a pinned charge-density wave is, instead, an artifact of too high a reflectance below 50 cm^{-1}. These high reflectances also cause unphysical negative conductivities at low fre-

quency. In this work, the conductivity at 35 cm^{-1} is a minimum.

ACKNOWLEDGMENTS

[1]L. B. Coleman, M. J. Cohen, D. J. Sandman, F. C. Yamagishi, A. F. Garito, and A. J. Heeger, Solid State Commun. 12, 1125 (1973).

[2]D. Jérome, A. Mazaud, M. Ribault, and K. Bechgaard, J. Phys. Lett. 41, L95 (1980).

[3]W.A. Little, Phys. Rev. 134, A1416 (1964).

[4]A. J. Heeger, in Chemistry and Physics of One-Dimensional Metals, edited by H. J. Keller (Plenum, New York, 1976).

[5]A. J. Berlinsky, Rep. Prog. Phys. 42, 1243 (1979).

[6]G. A. Toombs, J. Phys. Rep. C 40, 181 (1978).

[7]J. C. Gill, Contemp. Phys. 27, 37 (1986).

[8]M. J. Rice, C. B. Duke, and N. O. Lipari, Solid State Commun. 17, 1089 (1975).

[9]M. J. Rice, Phys. Rev. Lett. 37, 36 (1976).

[10]P. M. Grant, R. L. Greene, G. C. Wrighton, and G. Castro, Phys. Rev. Lett. 31, 1311 (1973).

[11]A. A. Bright, A. F. Garito, and A. J. Heeger, Phys. Rev. B 10, 1328 (1974).

[12]D. B. Tanner, K. D. Cummings, and C. S. Jacobsen, Phys. Rev. Lett. 47, 597 (1981).

[13]J. E. Eldridge and F. E. Bates, Phys. Rev. B 28, 6972 (1983).

[14]J. E. Eldridge, Phys. Rev. B 31, 5465 (1985).

[15]J. E. Eldridge (private communication).

[16]W. J. Gunning, S. K. Khanna, A. F. Garito, and A. J. Heeger, Solid State Commun. 21, 765 (1977).

[17]B. P. Gorshunov, G. V. Kozlov, A. A. Volkov, V. Železný, J. Petzelt, and C. S. Jacobsen, Solid State Commun. 60, 681 (1986).

[18]H. K. Ng, Ph.D. thesis, McMaster University, 1984 (unpublished).

[19]D. Bonn and T. Timusk (unpublished).

[20]N. O. Lipari, M. J. Rice, C. B. Duke, R. Bozio, A. Girlando, and C. Pecile, in Proceedings of the International Symposium on Atomic, Molecular, and Solid State Theory, Collision Phenomena, and Computational Methods, Sanibel Island, FL, 1977, edited by Per-Olov Lövdin (Wiley, New York, 1977).

[21]D. B. Tanner and C. S. Jacobsen, Mol. Cryst. Liq. Cryst. 85, 137 (1982).

[22]P. A. Lee, T. M. Rice, and P. W. Anderson, Phys. Rev. Lett. 31, 462 (1973); Solid State Commun. 14, 703 (1974).

[23]Cf. Fig. 2 in Ref. 27. Note that we do not find evidence for

a horizontal tangent as a function of ω for $\omega \rightarrow 0$.

[24]T. D. Holstein, Phys. Rev. 96, 535 (1954); P. B. Allen, Phys. Rev. B 3, 305 (1971).

[25]H. K. Ng, T. Timusk, and K. Bechgaard, Phys. Rev. B 30, 5842 (1984).

[26]M. J. Rice, Y. R. Wang, and E. J. Mele, Phys. Rev. B 40, 5304 (1989).

[27]J. Voit and E. J. Mele (unpublished).

[28]R. Bozio and C. Pecile, Solid State Commun. 37, 193 (1981).

[29]J. P. Pouget, S. K. Khanna, F. Denoyer, R. Comès, A. F. Garito, and A. J. Heeger, Phys. Rev. Lett. 37, 437 (1976); S. Kagoshima, T. Ishiguro, and H. Anzai, J. Phys. Soc. Jpn. 41, 2061 (1976).

[30]V. J. Emery, Phys. Rev. Lett. 37, 107 (1976); P. A. Lee, T. M. Rice, and R. A. Klemm, Phys. Rev. B 15, 2984 (1977).

[31]J. P. Pouget (private communication).

[32]T. Takahashi, D. Jérome, F. Masin, J. M. Fabre, and L. Giral, J. Phys. C 17, 3777 (1984).

[33]J. Sólyom, Adv. Phys. 28, 201 (1979).

[34]H. J. Schulz, Ph.D. thesis, Orsay, 1983 (unpublished).

[35]J. Voit and H. J. Schulz, Phys. Rev. B 37, 10068 (1988).

[36]J. P. Pouget, in Low-Dimensional Conductors and Superconductors, edited by D. Jérome and L. G. Caron (Plenum, New York, 1987).

[37]J. Voit, Synth. Met. 27, A41 (1988); see also Ph.D. thesis, Technische Universität München, 1986 (unpublished).

[38]See, e.g., G. Grüner, A. Zawadowski, and P. M. Chaikin, Phys. Rev. Lett. 46, 511 (1981).

[39]R. C. Lacoe, H. J. Schulz, D. Jérome, K. Bechgaard, and I. Johannsen, Phys. Rev. Lett. 55, 2351 (1985).

[40]P. Bak and V. J. Emery, Phys. Rev. Lett. 36, 978 (1976).

[41]H. Fukuyama and P. A. Lee, Phys. Rev. B 17, 535 (1978).

[42]W. J. Gunning, A. J. Heeger, I. F. Shchegolev, and S. P. Zolotukhin, Solid State Commun. 25, 981 (1978).

[43]J. Skov Pedersen and K. Carneiro, Rep. Prog. Phys. 50, 995 (1987).

[44]R. Comes, in Chemistry and Physics of One-Dimensional Metals, edited by H. J. Keller (Plenum, New York, 1976).

[45]A. Brau, P. Bruesch, J. P. Farges, W. Hinz, and D. Kuse, Phys. Status Solidi B 62, 615 (1974).

[46]M. J. Rice, L. Pietronero, and P. Bruesch, Solid State Commun. 21, 757 (1977).